

Geodesic congruences in warped spacetimes

Suman Ghosh ^{1*}, Anirvan Dasgupta ^{2,3 †} and Sayan Kar^{1,3 ‡}

¹*Department of Physics and Meteorology,*

Indian Institute of Technology, Kharagpur 721 302, India

²*Department of Mechanical Engineering,*

Indian Institute of Technology, Kharagpur 721 302, India

³*Centre for Theoretical Studies, Indian Institute of Technology, Kharagpur 721 302, India*

Abstract

In this article, we explore the kinematics of timelike geodesic congruences in warped five dimensional bulk spacetimes, with and without thick or thin branes. Beginning with geodesic flows in the Randall–Sundrum AdS (Anti de Sitter) geometry without and with branes we find analytical expressions for the expansion scalar and comment on the effects of including thin branes on its evolution. Later, we move on to congruences in more general warped bulk geometries with a cosmological thick brane and a time-dependent extra dimensional scale. Using analytical expressions for the velocity field, we interpret the expansion, shear and rotation (ESR) along the flows, as functions of the extra dimensional coordinate. The evolution of a cross-sectional area orthogonal to the congruence, as seen from a local observer’s point of view, is also shown graphically. Finally, the Raychaudhuri and geodesic equations in backgrounds with a thick brane are solved numerically in order to figure out the role of initial conditions (prescribed on the ESR) and spacetime curvature on the evolution of the ESR.

PACS numbers: 04.50.+h, 12.10.-g

* E-mail:suman@cts.iitkgp.ernet.in

† E-mail:anir@cts.iitkgp.ernet.in

‡ E-mail:sayan@cts.iitkgp.ernet.in

I. INTRODUCTION

Almost a century ago, in their pioneering research [1], Kaluza and Klein (KK) proposed unification of four dimensional gravity and electromagnetism in a five dimensional gravity framework. This proposal raised a fair amount of curiosity, interest and research activity among theoretical physicists, on the physics of extra dimensions. The idea of extra spatial dimensions appeared in a new incarnation with the advent of Superstring theories [2, 3]. The theoretical existence of branes in String theory eventually motivated the hypothesis that we may be living on an embedded, timelike submanifold (the brane) of a higher dimensional ($D > 4$) Lorentzian spacetime (warped or unwarped), as assumed in the so-called Arkani-Hamed–Dvali–Dimopoulos (ADD) [4, 5] and Randall–Sundrum (RS) [6] braneworld models.

The seminal work of Randall and Sundrum (RS) [6, 7] on warped braneworlds, published more than a decade ago, refers to the idea of the scale of the extra dimension being spacetime dependent, while addressing the issue of stability, in a two-brane scenario. In a single brane scenario or from a purely higher dimensional bulk perspective, the space-time dependence of the metric function(s) associated with the extra dimensional coordinate(s) basically imply that the scale of the extra dimension depends on the on-brane (four dimensional) spacetime coordinates. Except for a brief discussion on RS type models, we shall, in this article, mostly work with the single brane scenario and a five dimensional bulk.

In earlier papers [8, 9], geodesics in warped spacetimes have been investigated in detail. However, such a study of geodesics alone cannot tell us about the overall local behavior of a family of test particles, as observed in the neighbourhood of a freely falling observer. This motivates us to study the evolution of geodesic congruences. Since the appearance of *Raychaudhuri equations*, in 1955 [10], relativists have discussed and analysed its implications in various contexts. In its original incarnation, the Raychaudhuri equations provided the basis for the analysis of spacetime singularities in gravitation and cosmology [11]. For example, the equation for the expansion and the resulting theorem on geodesic focusing, is a crucial ingredient in the proofs of Penrose-Hawking singularity theorems [12, 13].

The kinematics of geodesic congruences is characterised by three kinematical quantities: isotropic expansion, shear and rotation (henceforth referred as ESR) [14–19], which evolve along the flow according to the Raychaudhuri equations. Though mostly quoted and used in the context of gravity, these equations by virtue of their geometric nature, have a much

wider scope in studying geodesic as well as non-geodesic flows in nature, which may possibly arise in diverse contexts (see [19] for some open issues). Two of the authors here have recently used these equations to investigate the kinematics of geodesic flows in stringy black hole spacetimes [20] and flows on flat and curved deformable media (including elastic and viscoelastic media) in detail [21, 22].

In this article, we attempt to understand the kinematics of geodesic flows in five dimensional warped bulk spacetimes with and without branes. In Section II we quickly recall the background spacetime geometries and geodesics. Section IIIA analyses flows in the RS geometry with and without branes. The ESR, as obtained from definitions, for a background with a thick brane are discussed in Section IIIB. Numerical solutions of the geodesic and Raychaudhuri equations are presented in IIIC. Finally, Section IV contains our conclusions and comments.

II. THE BULK SPACETIMES AND GEODESICS

The bulk spacetimes we work with are given by the line element [8] (η is the conformal time),

$$ds^2 = e^{2f(\sigma)} a^2(\eta) [-d\eta^2 + d\mathbf{X}^2] + b^2(\eta) d\sigma^2. \quad (2.1)$$

Table I, shows the chosen functional forms of $f(\sigma)$ (the warp factor), the cosmological [$a(\eta)$] and extra dimensional [$b(\eta)$] scale factors (following [8]). We mostly prefer to work with

$f(\sigma)$	$\{ a(\eta), b(\eta) \}$
$-\ln(\cosh k\sigma)$ Decaying warp factor	Set (A) $\{ 2\eta, 1 + \frac{1}{\eta} \}$ FRW (Radiation dominated) brane
$\ln(\cosh k\sigma)$ Growing warp factor	Set (B) $\{ \frac{1}{1-\eta}, 1 - \frac{\eta}{2} \}$ de Sitter brane

TABLE I: The four possible combinations of $f(\sigma)$, $a(\eta)$ and $b(\eta)$.

thick branes in order to avoid the discontinuities and delta functions which appear in the connection and curvature, for thin branes. However, as we will see later, in some special cases (e.g. Einstein spaces) one can indeed solve the Raychaudhuri equations consistently, with zero rotation and shear, in the presence of thin branes. It may be noted that these

models are assumed to represent the evolution of the universe beginning at a finite time when both the scales of visible and extra dimension were same.

The geodesic equations in the spacetime (2.1) are almost impossible to solve analytically. However, they may be recast as a dynamical system of coupled, ordinary, first order differential equations as given by Eqs 3.8-3.11 in [8]. Thus, for simple cases, knowing the first integrals one may directly determine the ESR.

III. RAYCHAUDHURI EQUATION AND ESR VARIABLES

A. Randall–Sundrum warp factor with and without branes

In Einstein spaces, $R_{AB} \sim g_{AB}$ and the equation for the expansion simplifies considerably if we assume the shear and rotation as zero. For the RSI scenario [6, 7] in the absence of any brane, the Raychaudhuri equation [14, 15] gives us

$$\frac{d\Theta}{d\lambda} + \frac{\Theta^2}{4} = \frac{\Lambda}{6M^3} \quad (3.1)$$

where, Λ is the bulk cosmological constant and M is the five dimensional Planck mass. With $\Theta = 4\frac{\dot{F}}{F}$ (notion of focusing is related to $F = 0$, $\dot{F} < 0$ at finite λ), leads to

$$\ddot{F} + k^2 F = 0, \quad \text{with} \quad k = \sqrt{\frac{-\Lambda}{24M^3}}, \quad (3.2)$$

Following [7], Λ is negative and Eq.3.2 has simple oscillatory solutions such as $c_1 \sin(k\lambda + c_2)$, which imply $\Theta = 4k \cot(k\lambda + c_2)$. Therefore, the nature of focusing or defocusing of geodesics in the bulk depends on the initial condition or the value of c_2 . However, this is the behavior of geodesic congruences in the bulk with no branes. If we introduce two 3-branes, the hidden brane (with positive tension $24M^3k$) at $\sigma = 0$ and the visible brane (with equal negative tension) at $\sigma = \pi$, Eq.3.2 becomes

$$\ddot{F} + [k^2 + 2k\{\delta(\sigma) - \delta(\sigma - \pi)\}] F = 0. \quad (3.3)$$

Using the following property of Dirac delta function

$$\delta(\sigma(\lambda)) = \sum_i \frac{\delta(\lambda - \lambda_i)}{|\dot{\sigma}(\lambda_i)|}, \quad (3.4)$$

and the first integral of the σ geodesic equation

$$\dot{\sigma} = \sqrt{C^2 e^{-2f} - 1} \quad \text{with} \quad f(\sigma) = -k|\sigma|, \quad (3.5)$$

we arrive at

$$\ddot{F} + [k^2 + k_1\delta(\lambda - \lambda_0) - k_2\delta(\lambda - \lambda_\pi)] F = 0, \quad (3.6)$$

where, $k_1 = \frac{2k}{\sqrt{C^2-1}}$, $k_2 = \frac{2k}{\sqrt{C^2e^{2k\pi}-1}}$, $\lambda_0 = \frac{\sec^{-1}C}{k}$ and $\lambda_\pi = \frac{\tan^{-1}\sqrt{C^2e^{2k\pi}-1}}{k}$. The solution of the above equation is given by [23]

$$F(\lambda) = c_1 \sin(k\lambda + c_2) + c_3 e^{-\alpha|\lambda-\lambda_0|} + c_4 e^{-\alpha|\lambda-\lambda_\pi|} \quad (3.7)$$

where c_1, c_2, c_3, c_4 are arbitrary constants. We then integrate the second order equation for F , around the neighborhood of λ_0 and λ_π to obtain two algebraic equations for c_1 and c_2 . The determinant condition for nontrivial solutions of c_1, c_2 yields the following transcendental equation,

$$(2\alpha - k_1)(2\alpha + k_2) + k_1 k_2 e^{-2\alpha(\lambda_\pi - \lambda_0)} = 0. \quad (3.8)$$

from which α can be obtained numerically. In our case, $\alpha \sim k_1/2$ is a good approximation (we have checked this with numerical solutions as well). Fig.1(a) shows (shaded regions) the domain of the parameters c_3/c_1 and c_4/c_1 (c_2 is taken to be zero), in cases where $F = 0$ at some finite value of λ between the two branes. Points on the boundaries of the shaded regions correspond to the occurrence of $F = 0$ at the location of the branes (i.e. $\lambda = \lambda_0, \lambda = \lambda_\pi$ and the corresponding σ through the function $\sigma(\lambda)$). In the lightly shaded region, $\dot{F} > 0$, which implies complete defocusing of geodesics ($\theta \rightarrow +\infty$) at finite λ , whereas in the darker region, $\dot{F} < 0$, i.e. geodesic focusing ($\theta \rightarrow -\infty$) is possible. Note that different values for c_2 will result in different parameter space diagrams involving the quantities c_3/c_1 and c_4/c_1 . Eq.3.7 leads to the modified expansion scalar, due to the presence of the branes, as given by

$$\Theta(\lambda) = 4 \frac{c_1 k \cos(k\lambda + c_2) - c_3 \alpha \operatorname{sgn}(\lambda - \lambda_0) e^{-\alpha|\lambda-\lambda_0|} - c_4 \alpha \operatorname{sgn}(\lambda - \lambda_\pi) e^{-\alpha|\lambda-\lambda_\pi|}}{c_1 \sin(k\lambda + c_2) + c_3 e^{-\alpha|\lambda-\lambda_0|} + c_4 e^{-\alpha|\lambda-\lambda_\pi|}}. \quad (3.9)$$

Due to the new integration constants, the behavior of geodesic congruences have become much richer. One such scenario is shown in Fig.1(b), where for specific values of these parameters, $c_1 = 1, c_3 = 1$ and $c_4 = -2$ which belongs to the dark shaded domain in Fig.1(a), gives rise to occurrence of congruence singularity in between the brane locations.

B. Calculating ESR from velocity field

One may derive analytic expressions for the ESR variables directly from the following definitions [14, 15] for the expansion Θ , the shear Σ_{AB} and the rotation Ω_{AB} , using the

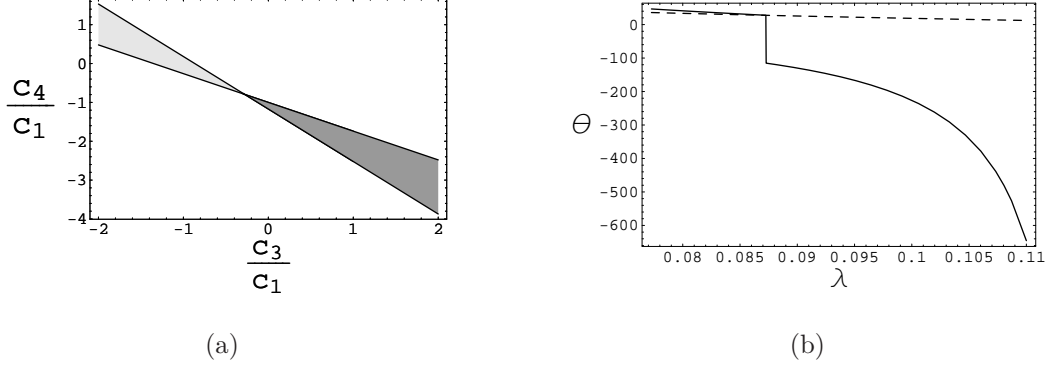


FIG. 1: (a) Phase diagram in the c_3/c_1 - c_4/c_1 plane. Points lying in the deeply (lightly) shaded region correspond to focusing (defocusing) of geodesics. (b) Evolution of expansion scalar in presence (continuous line) and in absence (dotted line) of two 3-branes with $c_1 = 1$, $c_3 = 1$ and $c_4 = -2$ which lies in the dark shaded region in (a). Specific values of the parameters are: $k = 12$, $C = 2$, $\lambda_0 = 0.087$ (1st brane location), $\lambda_\pi = 0.131$ (2nd brane location), $c_2 = 0$ and $\alpha = 6.9282$ (from Eq.3.8).

geodesic vector field components obtained in [8],

$$\Theta = \nabla_A u^A, \quad (3.10)$$

$$\Sigma_{AB} = \frac{1}{2} (\nabla_B u_A + \nabla_A u_B) - \frac{1}{n-1} h_{AB} \Theta, \quad (3.11)$$

$$\Omega_{AB} = \frac{1}{2} (\nabla_B u_A - \nabla_A u_B). \quad (3.12)$$

Here, n is the dimension of spacetime and $h_{AB} = g_{AB} \pm u_A u_B$ is the projection tensor (the plus sign is for timelike curves whereas the minus one is for spacelike ones) and $u_A u^A = \mp 1$. Let us now obtain the ESR for some specific cases (for thick branes), where we take one or two of the metric functions as constants.

1. Case 1: $a(\eta) = b(\eta) = \text{constant}$

Here, with only a non-constant $f(\sigma)$ present in 2.1, the velocity field components for timelike geodesics are

$$u^\alpha = C_\alpha e^{-2f} \quad \text{where } \alpha = 0, 1, 2, 3 \quad (3.13)$$

$$u^4 = \sqrt{C^2 e^{-2f} - 1} \quad \text{where } C^2 = C_0^2 - \sum_{i=1}^3 C_i^2, \quad (3.14)$$

where the C_α 's are integration constants, which are constrained by the fact that u^4 has to be real valued.

According to the definitions Eq.3.10 - Eq.3.12, the expansion scalar and the other ESR variables for a congruence of timelike geodesics, written as functions of σ , give us,

$$\Theta = \frac{3C^2 e^{-2f} - 4}{\sqrt{C^2 e^{-2f} - 1}} f', \quad (3.15)$$

$$\Sigma^2 = \Sigma_{AB} \Sigma^{AB} = \frac{3C^4 e^{-4f} f'^2}{4(C^2 e^{-2f} - 1)} \quad \text{and} \quad \Omega_{AB} = 0 \forall A, B. \quad (3.16)$$

For the chosen growing and decaying warp factors respectively, the expansion scalar becomes

$$\Theta_+ = \frac{3C^2 \operatorname{sech}^2 \sigma - 4}{\sqrt{C^2 \operatorname{sech}^2 \sigma - 1}} \tanh \sigma \quad \text{and} \quad \Theta_- = -\frac{3C^2 \cosh^2 \sigma - 4}{\sqrt{C^2 \cosh^2 \sigma - 1}} \tanh \sigma. \quad (3.17)$$

It can be easily seen that, for $\dot{\sigma} > 0$ and $C > 1$, $\Theta_\pm \rightarrow -\infty$ as σ increases. Therefore a geodesic congruence singularity arises in both the cases. With Θ_+ , if $C > \sqrt{4/3}$, initially the expansion remains positive but eventually geodesics meet exactly at the boundary of the accessible domain along the extra dimension because the velocity component along σ , u^4 , which appears in the denominator in the expression for Θ , vanishes at that point (and also changes sign). With Θ_- , the geodesic congruence singularity appears as $\sigma \rightarrow \infty$. For $\dot{\sigma} < 0$ an exactly similar behavior is obtained. From the nature of corresponding geodesics (see [8]), we note that Θ_+ experiences a finite time singularity (i.e. finite λ as well as finite σ) but Θ_- becomes singular at finite λ but $\eta, \sigma \rightarrow \infty$.

To understand how geodesic congruences behave in all the abovementioned scenarios, let us consider the evolution of the projections of the cross-sectional area orthogonal to the flow lines, of a congruence of four geodesics, on different two dimensional surfaces. This is done by numerically solving

$$u^C \nabla_C B_{AB} = -B_{AC} B_B^C - R_{ACBD} u^C u^D. \quad (3.18)$$

$$\xi^A_{;B} u^B = B^A_B \xi^B \quad (3.19)$$

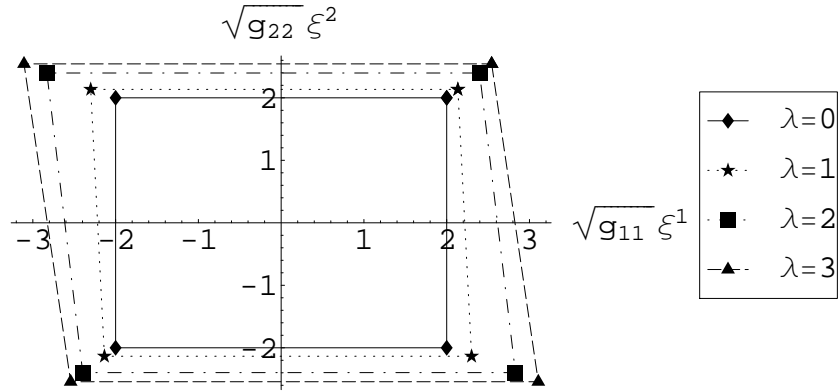
along with the geodesic equations. Here, $B_{AB} = \nabla_B u_A$ is the gradient of velocity field and ξ^A represents the separation between two neighboring geodesics. Eq.3.19 is essentially the evolution equation for the deviation vector. To see the evolution from a local observer's viewpoint, we have to express the tensorial quantities in the frame basis. The metric tensor in coordinate basis and frame basis are related as

$$g^{AB} = e^A_a e^B_b \eta^{ab}, \quad (3.20)$$

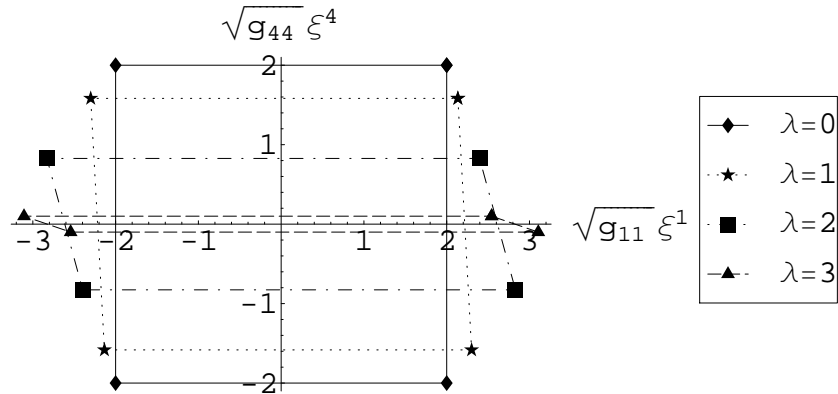
where the vierbein field, e_a^A , has two indices, “ A ” labels the general spacetime coordinate (w.r.t. the coordinate basis) and “ a ” labels the local Lorentz spacetime or local laboratory coordinates (w.r.t. the frame basis). The tensorial components in these two bases are related as

$$\xi^A = e_a^A \xi^a. \quad (3.21)$$

In the frame basis, we set the initial conditions such that, at $\lambda = 0$, the projected area has the shape of a square in the $\sqrt{g_{11}}\xi^1$ - $\sqrt{g_{22}}\xi^2$ plane or in the $\sqrt{g_{11}}\xi^1$ - $\sqrt{g_{44}}\xi^4$ plane where ξ 's are essentially solutions of Eq.3.19. Fig.2 shows the evolution of the area elements as λ increases. The origin represents the location of the observer. We have chosen initial conditions such that all components of the rotation vanish.



(a) Evolution of the projected square element on $\sqrt{g_{11}}\xi^1$ - $\sqrt{g_{22}}\xi^2$ plane

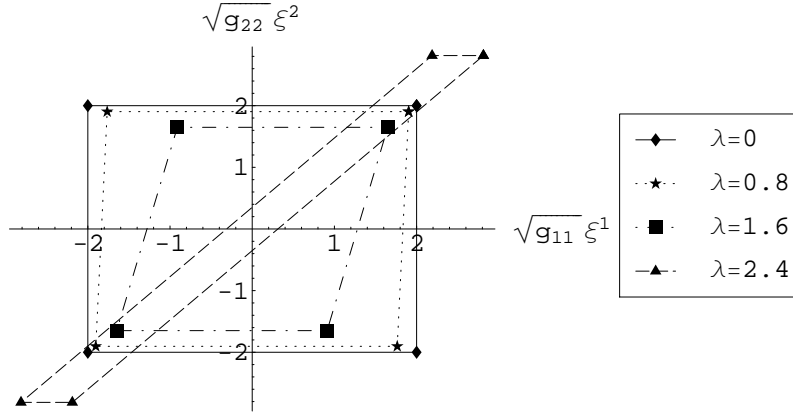


(b) Evolution of the projected square element on $\sqrt{g_{11}}\xi^1$ - $\sqrt{g_{44}}\xi^4$ plane

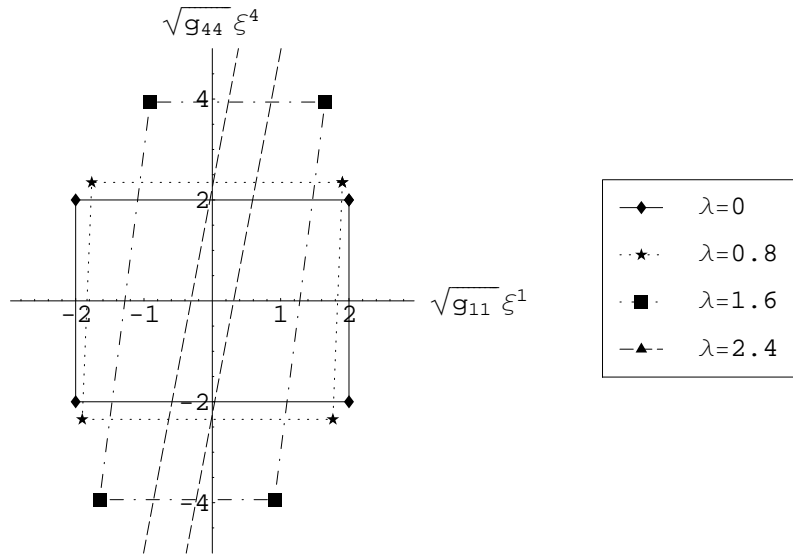
FIG. 2: Evolution of different 2D surface elements in Case 1 in presence of a growing warp factor

Fig.2 shows how a projected 2D square element evolves, in a static bulk, in presence

of a growing warp factor. In Fig.2(a), the initial square area (at $\lambda = 0$) in the $\sqrt{g_{11}}\xi^1$ - $\sqrt{g_{22}}\xi^2$ plane expands and distorts slightly and converges on a parallelogram at $\lambda \sim 3.14$. In Fig.2(b), however the area in the $\sqrt{g_{11}}\xi^1$ - $\sqrt{g_{44}}\xi^4$ plane shrinks, distorts and converges on the $\sqrt{g_{11}}\xi^1$ axis at $\lambda \sim 3.14$, clearly suggesting focusing along the extra dimension. The effect of shear is evident from the evolution of the shape of the area.



(a) Evolution of the projected square element on $\sqrt{g_{11}}\xi^1$ - $\sqrt{g_{22}}\xi^2$ plane



(b) Evolution of the projected square element on $\sqrt{g_{11}}\xi^1$ - $\sqrt{g_{44}}\xi^4$ plane

FIG. 3: Evolution of different 2D surface elements in Case 1 in presence of a decaying warp factor.

On the other hand, Fig.3 corresponds to the scenario where the warp factor is of decaying

type. In Fig.3(a), shrinking of the area element is quite prominent whereas in Fig.3(b) it is not so. However, in both the figures, the square area becomes more and more parallelogram shaped and eventually converge on a line $\sqrt{g_{11}}\xi^1 \propto \sqrt{g_{22}}\xi^2$ or $\sqrt{g_{11}}\xi^1 \propto \sqrt{g_{44}}\xi^4$ as $\lambda \rightarrow \infty$.

The nature of evolution of the square elements is therefore a distinguishing feature between bulk universes with growing and decaying warp factors. It is worth mentioning here that, to a brane based observer, only the evolution depicted in Fig.2(a) or Fig.3(a) will be visible whereas congruence singularities realised in Fig.2(b) or Fig.3(b) will remain unnoticed. In a way, therefore, one can find the nature of warping as well as the existence of extra dimensions from the evolution pattern of cross-sectional area elements.

2. Case 2: $f(\sigma)=\text{constant}$

In this case, with only non-constant $a(\eta)$, $b(\eta)$ present in 2.1, the velocity field components for timelike geodesics are

$$\begin{aligned} u^i &= \frac{C_i}{a^2}, & u^4 &= \frac{C_4}{b^2}, \\ u^0 &= \sqrt{\frac{1}{a^2} + \sum_{i=1}^3 \frac{C_i^2}{a^4} + \frac{C_4^2}{a^2 b^2}} \end{aligned} \quad (3.22)$$

We can calculate the expansion scalar which turns out to be,

$$\Theta = -\frac{1}{u_0} \left[3\frac{\dot{a}}{a} + 2\sum_i \frac{C_i^2 \dot{a}}{a^3} + \frac{3C_4^2 \dot{a}}{ab^2} + \frac{\dot{b}}{b} + \sum_i \frac{C_i^2 \dot{b}}{a^2 b} \right]. \quad (3.23)$$

As done before one can also find the components of the shear tensor (not shown here). The rotation tensor components are zero, as is evident from the velocity field.

In case of Set(A) [as given in Table I], the geodesics become parallel as $\eta \rightarrow \infty$. This is because, with a FRW (radiation dominated) brane, the expansion of the universe itself slows down with increasing η (it is worth mentioning here that as the cosmological evolution is assumed to begin at a finite η , the past singularity will not appear here since it corresponds to $\eta = 0$ and falls outside the domain of η for the models considered in this article). For Set(B) [see Table I], the geodesics spread apart at an ever increasing rate with increasing η – this is due to very rapid (exponential in real time) expansion of the universe. In both these cases geodesic focusing is not achieved. On the other hand, as noted in the previous subsection, geodesic singularities are unavoidable when a non-constant warp factor

is assumed. Therefore, it should be interesting to see how these two apparently opposite features compete with each other when we consider the full braneworld geometry with all three non-constant metric functions present.

We end this subsection by trying to figure out the individual effect of the dynamic nature of $b(\eta)$. Assuming $a(\eta)$ as constant in Eq.3.23 we get,

$$\Theta = \frac{(1 + \sum_i C_i^2) \dot{b}}{\sqrt{(1 + \sum_i C_i^2) b^2 + C_4^2}}. \quad (3.24)$$

In our models \dot{b} is negative and as η increases it tends to zero. For the $b(\eta)$ of Set(A), Θ tends to zero i.e. geodesics become parallel while for Set(B) it converges to a finite value which implies that the geodesics keep moving away from each other at an approximately steady rate. So, with only a $b(\eta)$, in both the above Sets (A) and (B), geodesic focusing never happens. It is interesting to note that even if $b(\eta) \rightarrow 0$ i.e. size of the extra dimension becomes singular the expansion scalar remains finite as long as \dot{b} is finite. Therefore we expect $b(\eta)$ to play a role only in introducing a scaling effect. This will become clearer in the next section, when we consider the general scenario where all the three non-constant metric functions are considered.

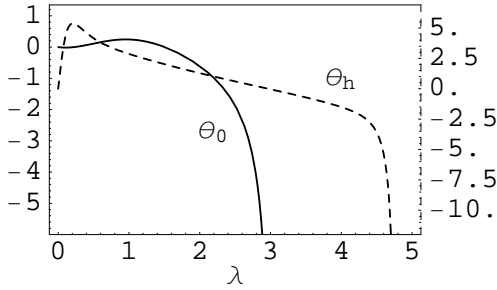
One may ask—what about analytic expressions for the kinematic variables in the general case? Analytic expressions for the first integrals of the geodesic equations with non-constant $f(\sigma)$ and $a(\eta)$ can be found easily. However, the ESR as obtained from the definitions (Eq.3.10-3.12) are functions of σ , η and cannot be reduced to explicit functions of λ alone. This happens because we do not know how $\sigma(\lambda)$ and $\eta(\lambda)$ are related analytically. Thus, the above two subcases are the only ones where one can find useful, closed-form analytic expressions for the ESR, directly from the velocity field.

C. Numerical solutions

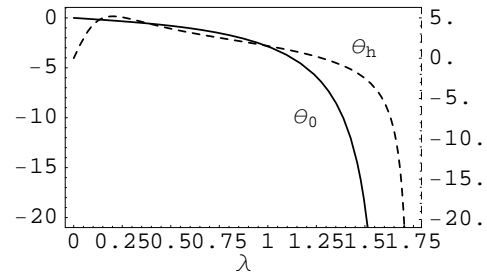
Here, we numerically solve Eq.3.18 simultaneously with the geodesic equation for different combinations of the metric functions, in order to understand the interplay amongst all the terms appearing in the Raychaudhuri equations [14, 15]. The effect of the shear and rotation on the expansion are mutually opposite. Thus, the rotation may play a role in avoiding/delaying congruence singularities. On the other hand, the curvature term $R_{AB}u^A u^B$ also has a significant effect on ESR profiles through its large positive or negative value at a

given spacetime point.

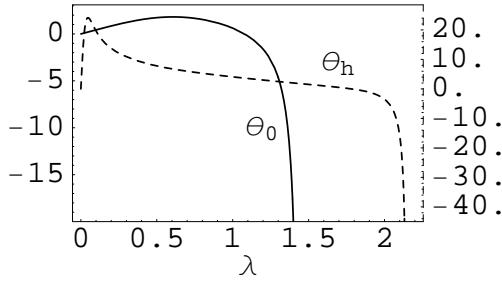
We have analysed each case for two types of initial conditions – one with zero initial rotation and one with very high initial rotation, keeping initial Θ and Σ_{AB} as zero. Non-zero initial values for Ω_{AB} are chosen such that $\Omega_{AB}u^B = 0 = u^A\Omega_{AB}$ at $\lambda = 0$. Initial velocities for cases involving Set(A) scale factors are taken as $\{0.728, 0.1, 0.1, 0.1, 0.5\}$, whereas for Set(B), it is assumed as $\{1.1314, 0.1, 0.1, 0.1, 0.5\}$ so that the timelike constraint is satisfied. In Fig.4, we present the evolution of the expansion scalar for the different scenarios mentioned in Table I.



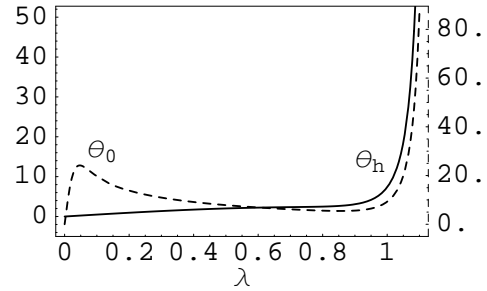
(a) With $f(\sigma) = \log(\cosh \sigma)$, $a(\eta) = 2\eta$ and $b(\eta) = 1 + 1/\eta$



(b) With $f(\sigma) = -\log(\cosh \sigma)$, $a(\eta) = 2\eta$ and $b(\eta) = 1 + 1/\eta$



(c) With $f(\sigma) = \log(\cosh \sigma)$, $a(\eta) = 1/(1 - \eta)$ and $b(\eta) = 1 - \eta/2$



(d) With $f(\sigma) = -\log(\cosh \sigma)$, $a(\eta) = 1/(1 - \eta)$ and $b(\eta) = 1 - \eta/2$

FIG. 4: Nature of expansion scalar for different cosmological braneworld scenarios with two different sets of initial conditions. The subscripts 0 (*h*) correspond to zero (high) initial rotation.

In the presence of a growing warp factor, a FRW (radiation dominated) brane and an asymptotically static extra dimension, geodesic congruences without any initial rotation, expand slowly at first but later become focused at a finite λ , as observed in Fig.4(a). The shear (Σ^2) is found to grow indefinitely (figure not shown). When high initial rotation is

introduced, the congruence diverges for a very short while but eventually the geodesics get focused again at another finite but larger value of λ . Though rotation increases at late times, it is always dominated by shear, which grows even faster. Initial rotation only succeeds in delaying the focusing. The curvature term, as we note, is not an important factor here.

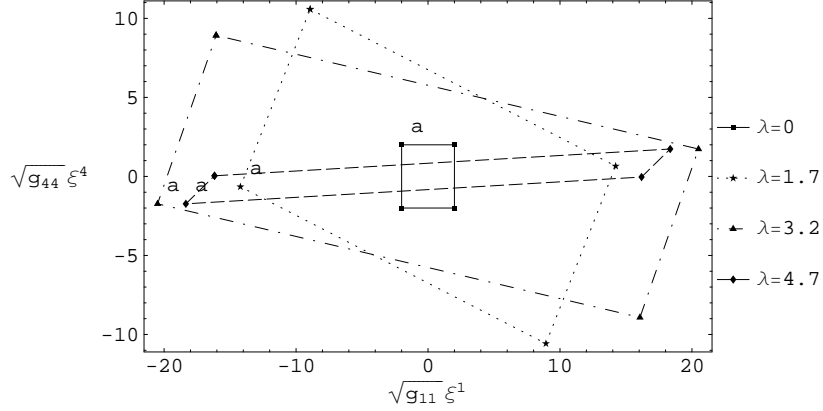
In contrast, Fig.4(b) shows that, in the presence of a decaying warp factor, a FRW (radiation dominated) brane and an asymptotically static extra dimension, the geodesics, without any initial rotation, do come closer to each other monotonically, but focus only at $\sigma \rightarrow \infty$. As before, the shear grows indefinitely. When high initial rotation is introduced, the congruence expands initially but eventually geodesics tend to focus again asymptotically. The curvature term becomes large positive valued and thus always seems to help in the occurrence of congruence singularities.

Fig.4(c) represents almost the same behavior as seen in Fig.4(a). However, here the large initial rotation decays down very quickly. The physical reason behind this is the very fast expansion of spacetime that smears out all the initial rotation components.

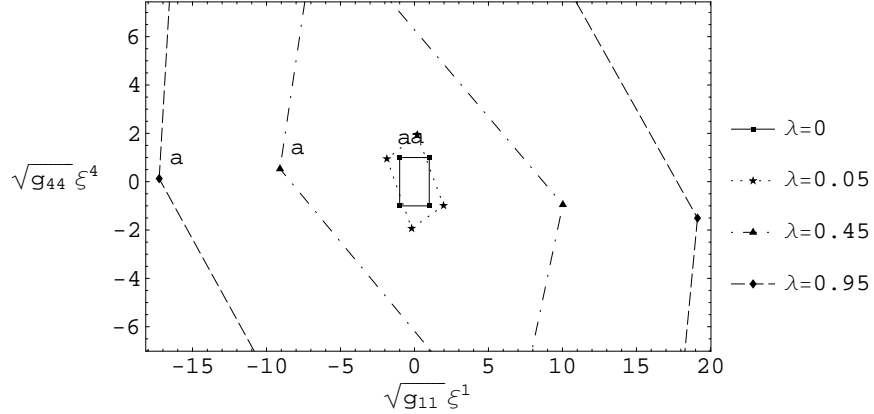
On the other hand, in the presence of a decaying warp factor, a de Sitter brane with an asymptotically static extra dimension, in Fig.4(d), we have an example where geodesics are defocused irrespective of the initial rotation. Even though it seems that at late times shear totally dominates over rotation, it is the curvature term in the Raychaudhuri equation that becomes dominant and causes the defocusing. Remember that, with $a(\eta) = b(\eta) = \text{constant}$, congruence singularity was inevitable. On the other hand, we have observed that initially the curvature term is very small. This implies that, in this case, a high enough initial negative expansion should lead to a congruence singularity at a finite λ (before the curvature term becomes dominant). This behavior has been checked with an initial expansion, $\Theta = -30$ (figure not shown).

From the results in Fig.4, one can draw some general conclusions about the nature of the ESR variables. Congruence singularity is inevitable (irrespective of the initial rotation) in the cases addressed in Fig.4(a) and Fig.4(c). This is because, in the presence of growing warp factor, the geodesics have a turning point in the extra dimension. This forces the congruence singularity to occur. Fig.4(b) represents a case where the geodesics are not bounded. Even in this case, a high initial expansion cannot make the congruence to diverge. On the other hand, the geodesics are divergent when $f(\sigma) = -\log(\cosh \sigma)$, $a(\eta) = 1/(1 - \eta)$ and $b(\eta) = 1 - \eta/2$ [Fig.4(d)], which corresponds to a negatively warped and exponentially

expanding brane. Here, it is interesting to note that the defocusing occurs because of the curvature term which becomes dominant and large negative, and has nothing to do with the initial rotation. Therefore, one can say that this defocusing is purely an effect of the spacetime geometry.



(a) Evolution of 2D surface elements for $f(\sigma) = \log(\cosh \sigma)$, $a(\eta) = 2\eta$ and $b(\eta) = 1 + 1/\eta$ with $\Theta = \Sigma^2 = 0$ and $\Omega^2 \sim 54$ at $\lambda = 0$.



(b) Evolution of 2D surface elements for $f(\sigma) = -\log(\cosh \sigma)$, $a(\eta) = 1/(1 - \eta)$ and $b(\eta) = 1 - \eta/2$ with $\Theta = \Sigma^2 = 0$ and $\Omega^2 \sim 1080$ at $\lambda = 0$.

FIG. 5: Evolution of the projected square elements on $\sqrt{g_{11}}\xi^1 - \sqrt{g_{44}}\xi^4$ plane.

Let us now look at the evolution of a congruence of geodesics from the local observer's point of view and see how the ESR profiles, plotted in Fig. 4, are realised. As done earlier, here also we have plotted the evolution of square elements, orthogonal to the congruence of the timelike geodesics, projected on $\sqrt{g_{11}}\xi^1 - \sqrt{g_{44}}\xi^4$ planes. These plots provide a different

perspective of the evolution since they involve different shear and rotation tensor components. We have labeled one point of each area element (the one in the second quadrant, initially) as “a”. Following the location of this labeled point on future quadrilaterals (with increasing λ) one can see the effect of rotation.

Fig.5(a) corresponds to the evolution of the dashed curve in Fig.4(a) (i.e. in presence of a growing warp factor). In Fig.5(a), shrinking of the area element after an initial expansion, increase in the amount of shear after a decrease in the middle and a quick decrease in rotation are more clearly visible.

Fig.5(b) represents the evolution of the dashed curve in Fig.4(d) (i.e. in presence of a decaying warp factor). The area of the quadrilateral keeps on increasing with λ . Effect of high initial rotation is prominent, so is its rapid decrease. Effect of shear in Fig.5(b) matches with the profile of Fig.4(d). As mentioned earlier, these qualitatively different ESR evolutions are in one to one correspondence with different models. Therefore, loosely speaking, the pictorial visualisation provides pointers toward possible verification of those models, though much more needs to be done in order to arrive at explicit verifiable signatures.

Warp factor $e^{2f(\sigma)}$	Constant $a(\eta), b(\eta)$ (Analytical results)	$a(\eta) = 2\eta, b(\eta) = 1 + 1/\eta$ (FRW Radiation dominated)	$a(\eta) = 1/(1 - \eta), b(\eta) = 1 - \eta/2$ (de Sitter)
Growing	Congruence singularity at finite σ	Congruence singularity at finite σ [Fig.4(a)]	Congruence singularity at finite σ [Fig.4(c)]
Decaying	Congruence singularity at $\sigma \rightarrow \infty$	Congruence singularity at $\sigma \rightarrow \infty$ [Fig.4(b)]	Defocusing at $\sigma \rightarrow \infty$ [Fig.4(d)] or congruence singularity at finite σ for large, -ve initial Θ
Constant	–	No congruence singularity	No congruence singularity

TABLE II: Summary of behaviour of geodesic congruences for different metric coefficients

IV. DISCUSSION

We began by considering geodesic flows in the RS background. Without branes congruence singularities always occur whereas with two branes, the expansion profile indicates how focusing/defocusing can occur in the spacetime between the branes.

Later, we analyse geodesic flows in a bulk geometry with a thick brane. Using first integrals of geodesic motion, analytic expressions for the kinematic variables are obtained. We show how differences arise as we change the warp factor from growing to decaying or when we do not have any warping but retain the time-evolving cosmological and extra dimensional scales.

Further, we numerically solve the Raychaudhuri and geodesic equations to obtain the expansion, shear, rotation and demonstrate the role of initial conditions on their evolution. With $a(\eta) = \eta$, a growing warp factor leads to a finite η (and σ) congruence singularity whereas for a decaying warp factor, geodesics are focused at η (and σ) $\rightarrow \infty$. For a de Sitter universe, a decaying warp factor may fail to focus the geodesics (due to the large negativity of the curvature term in the Raychaudhuri equation), though this is not the case with a growing warp factor. When the curvature effect is relatively small, a congruence singularity can still arise but for high enough negative initial expansion. The effect of initial rotation, on the ESR profiles, especially the expansion scalar, is found to be quantitative. Focusing without and with initial rotation yields similar results, though with large initial rotation, geodesics tend to spread for a while (focusing at larger λ value). All our conclusions are summarised in Table II.

For a visual perspective, we have shown snap-shots of the evolution of a square element orthogonal to a geodesic congruence, from a local observer's point of view. The evolution of the expansion, shear and rotation, along the congruences become more explicit through these figures.

The effect of $b(\eta)$ seems to be largely quantitative since, in our models, as λ evolves $b(\eta)$ tends to a static value with a deceleration.

It may be asked—what relevance, if any, does a congruence singularity have in the context of realistic scenarios? After all, congruence singularities are not real spacetime singularities where curvatures diverge. Here, we are tempted to draw an analogy from null geodesic congruences, for which congruence singularities are nothing but the well-studied caustics where optical intensities get magnified immensely. Similarly, in the case of timelike geodesics, we may end up with accretion-like effects resulting out of matter accumulation in the neighborhood of a point. For instance, our visualisation analyses do show how the square elements change shape, get rotated because of variations in the metric functions. We may contemplate such accretion effects for flows around brane-world black holes [24] and in such situations,

it will become necessary to pursue a line of thought very similar to what we have followed in this article.

Acknowledgments

SG thanks Council for Scientific & Industrial Research (CSIR), India for providing financial support and Centre for Theoretical Studies, IIT Kharagpur, India for allowing him to use its research facilities.

-
- [1] T. Kaluza, *Sitzungsber. Preuss. Akad. Wiss. Berlin. (Math. Phys.)*, 966-972 (1921); O. Klein, *Z. Phys.* **37** (1926) 895
 - [2] M. S. Green, J. H. Schwarz and E. Witten, *Superstring theory* (Cambridge University Press, UK, 1987); J. Polchinski, *String theory* (Cambridge University Press, UK, 1997).
 - [3] I. Antoniadis, *Phys. Lett. B* **246** (1990) 377.
 - [4] N. Arkani-Hamed, S. Dimopoulos, G. Dvali, *Phys. Lett. B* **429**, 263-272 (1998); N. Arkani-Hamed, S. Dimopoulos, G. Dvali, *Phys. Rev. D* **59**, 086004 (1999).
 - [5] I. Antoniadis, N. Arkani-Hamed, S. Dimopoulos and G. R. Dvali, *Phys. Lett. B* **436** (1998) 257 [arXiv:hep-ph/9804398].
 - [6] L. Randall and R. Sundrum, *Phys. Rev. Lett.* **83**, 3370 (1999).
 - [7] L. Randall and R. Sundrum, *Phys. Rev. Lett.* **83**, 4690 (1999).
 - [8] S. Ghosh, S. Kar and H. Nandan, *Phys. Rev. D* **82**, 024040 (2010).
 - [9] S. S. Seahra, *Phys. Rev.* **D68**, 104027 (2003).
 - [10] A. K. Raychaudhuri, *Phys. Rev.* **98**, 1123 (1955);
 - [11] S. W. Hawking and G. F. R. Ellis, *The large scale structure of spacetime* (Cambridge University Press, Cambridge, UK, 1973).
 - [12] R. Penrose, *Phys. Rev. Lett.* **14**, 57 (1965).
 - [13] S. W. Hawking, *Phys. Rev. Lett.* **15**, 689 (1965); *ibid.* **17**, 444 (1966).
 - [14] E. Poisson, *A relativists' toolkit: the mathematics of black hole mechanics* (Cambridge University Press, UK, 2004).
 - [15] R. M. Wald, *General Relativity* (University of Chicago Press, Chicago, USA, 1984).

- [16] P. S. Joshi, *Global aspects in gravitation and cosmology* (Oxford University Press, Oxford, UK, 1997).
- [17] G. F. R. Ellis in *General Relativity and Cosmology, International School of Physics, Enrico Fermi–Course XLVII* (Academic Press, New York, 1971).
- [18] I. Ciufolini and J. A. Wheeler, *Gravitation and inertia* (Princeton University Press, Princeton, USA, 1995).
- [19] S. Kar and S. SenGupta, *Pramana* **69**, 49 (2007) and references therein; S. Kar, *Resonance, Journal of Science Education* **13**, 319 (2008).
- [20] A. Dasgupta, H. Nandan and S. Kar, *Phys. Rev. D* **79** 124004 (2009).
- [21] A. Dasgupta, H. Nandan and S. Kar, *Annals of Physics* **323**, 1621 (2008).
- [22] A. Dasgupta, H. Nandan and S. Kar, *Int. J. of Geom. Meth. Mod. Phys.* **6(4)** (2009).
- [23] T. C. Scott and R. B. Mann, *General Relativity and Quantum Mechanics: Towards a Generalization of the Lambert W Function*, AAEECC (Applicable Algebra in Engineering, Communication and Computing), vol. 16, no. 6, (2006) [arXiv:math-ph/0607011v2].
- [24] C. S. J. Pun, Z. Kovacs and T. Harko, *Phys. Rev. D* **78** (2008) 084015